

NONLINEAR DYNAMICS AND DISSIPATION OF VORTEX LINES DRIVEN BY STRONG RF FIELDS*

W.P.M.R Pathirana[†], Alex Gurevich

Center for Accelerator Science, Old Dominion University, Norfolk, USA

Abstract

Trapped vortices can contribute significantly to a residual surface resistance of superconducting radio frequency (SRF) cavities but the nonlinear dynamics of flexible vortex lines driven by strong rf currents has not been yet investigated. Here we report extensive numerical simulations of large-amplitude oscillations of a trapped vortex line under the strong rf magnetic field. The rf power dissipated by an oscillating vortex segment driven by the rf Meissner currents was calculated by taking into account the nonlinear vortex line tension, vortex mass and a nonlinear Larkin-Ovchinnikov viscous drag force. We calculated the field dependence of the residual surface resistance R_i and showed that at low frequencies $R_i(H)$ increases with H but as the frequency increases, $R_i(H)$ becomes a nonmonotonic function of H which decreases with H at higher fields. These results suggest that trapped vortices can contribute to the extended $Q(H)$ rise observed on the SRF cavities.

INTRODUCTION

The field performance and losses of the SRF accelerator cavities are quantified by the quality factor $Q(H)$ which is inversely proportional to the surface resistance $R_s(R)$. At low RF fields $R_s = R_{BCS} + R_i = (Af^2/T) \exp(-\Delta/k_B T) + R_i$ contains the BCS contribution due to thermally activated quasiparticles and the residual resistance R_i which remains finite as $T \rightarrow 0$. The best Nb resonator cavities can have $Q \approx 10^{10} - 10^{11}$ with $R_s \approx 10 - 30$ n Ω and $R_i \approx 2 - 10$ n Ω at 2 K [1–3]. The residual resistance gives a significant contribution to the RF losses (about $\geq 20\%$ for Nb and $\geq 50\%$ for Nb₃Sn at 2K [4]), so the dependence of R_i on the magnetic field H and frequency f is of much interest.

One of the essential contributions to R_i comes from trapped vortices generated during the cavity cool down through the critical temperature T_c at which the lower critical field $H_{c1}(T)$ vanishes [5–13]. In this case even small stray fields $H > H_{c1}(T)$ such as unscreened earth magnetic field can produce vortices in the cavity. During the subsequent cooldown to $T \approx 2$ K some of these vortices exit the cavity but some get trapped by the material defects such as non-superconducting precipitates, network of dislocations or grain boundaries.

RF power generated by oscillating flexible vortices under weak RF field has been addressed theoretically [6, 14] and in a simplified model [15] which neglects the essential line tension of the vortex. Quasi-static power generated by single

vortices parallel to the surface [16] and perpendicular vortices in the collective pinning theory [4] has been recently calculated. However, the nonlinear dynamics of trapped vortex lines perpendicular to the surface under strong rf currents has not been addressed. In this work we calculate the field and frequency dependence of R_s due to a trapped vortex line under the strong rf magnetic field, taking into account the nonlinear vortex line tension, vortex mass and nonlinear viscous drag force. Our results show that $R_i(H)$ can decrease with the RF field at higher frequencies.

DYNAMICS OF A TRAPPED VORTEX UNDER STRONG RF FIELD

Consider a single vortex pinned by a materials defect as shown in the Figure 1. The motion of a vortex is completely

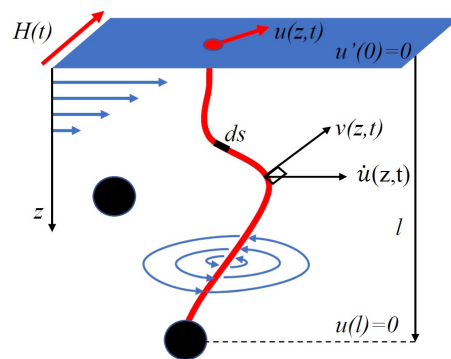


Figure 1: A flexible vortex shown by the read line driven by the rf surface current. The black dots represent pinning centers such as nonsuperconducting precipitates.

determined by its horizontal displacement $u(z,t)$ as a function of z and t . Here the tip of the vortex is perpendicular to the surface [14] so that $u'(0) = 0$. We did simulations for defects with different pinning forces, but here we only present results for the case when the other end of the vortex segment is fixed by a strong pin at $l = 0$ resulting in the second boundary condition $u(l) = 0$ [6].

The dynamic equation for the local velocity $v(z,t)$ normal to the curved vortex line can be written in the form:

$$m\dot{v} + \eta(v)v = \frac{\epsilon}{R} - \frac{\phi_0 H}{\lambda} e^{-z/\lambda} \sin(\omega t), \quad (1)$$

where λ is the London penetration depth, m is the vortex mass, $\eta(v)$ is the nonlinear viscosity, $\epsilon = \phi_0^2 \ln(\kappa + 0.5)/4\pi\mu_0\lambda^2$ is the vortex line energy, $\kappa = \lambda/\xi$ is the Ginzburg-Landau parameter, ξ is the coherence length, and

* This work was supported by NSF under Grant 100614-010 and Grant 1734075.

[†] mwali003@odu.edu

R^{-1} is the local curvature of the vortex line. The perpendicular velocity of the vortex $v(z, t)$ is related by the parallel velocity component $\dot{u}(z, t)$ along x by \dot{u} by $v(z, t) = \dot{u}\sqrt{1 + u'^2}$. Equation (1) represents the balance of four major forces acting perpendicular to the vortex line: the inertial and the viscous drag forces in the left hand side are balanced by the elastic force ϵ/R and the Lorentz force of the RF current in the right hand side. The line tension force ϵ/R in which the local curvature $R^{-1} = u''(1 + u'^2)^{-3/2}$ depends on the shape of the vortex line accounts for a nonlinear elasticity of vortices in the London model [14]. Detailed calculations of nonlinear deformation of vortices described by the time-dependent GL equations were performed in Ref. [17].

Viscous drag force $F_\eta = \eta v$ results from eddy currents of quasiparticles in the vortex core [18]. At small velocities the viscous drag coefficient can be estimated from the Bardeen-Stephen model which gives $\eta_0 = B_{c2}\phi_0/\rho_n$ for superconductors with a short mean free path $\ell < \xi_0$, where ρ_n is normal-state resistivity $B_{c2} = \phi_0/2\pi\xi^2$ is the upper critical field and ϕ_0 is the magnetic flux quantum. However, as the vortex velocity increases $\eta(v)$ becomes dependent on v . For instance, Larkin and Ovchinnikov (LO) [19] have shown that the damping coefficient $\eta(v)$ decreases with v because the number of normal quasiparticles in the core decreases as they diffuse away from the core at high velocities [17, 19, 20]. In this case the nonlinear drag force can be written in the form [19]:

$$F_\eta = \frac{\eta_0 v}{1 + v^2/v_0^2} \quad (2)$$

The critical LO velocity $v_0 \propto (D/\tau_\epsilon)^{1/2}$ in Eq. (2) depends on the energy relaxation time τ_ϵ and diffusivity D of normal quasiparticles [19]. Here $v_0(T)$ vanishes at T_c but decreases at low temperatures $T \ll T_c$, where $\tau_\epsilon(T)$ increases rapidly at T decreases [20]. A similar velocity dependence of $F_\eta(V)$ occurs due to electron overheating in the moving vortex [16].

The force $F_\eta(v)$ is a nonmonotonic function of v which reaches maximum $F_{max} = \eta_0 v_0/2$ at the vortex velocity $v_{max} = v_0$. As a result, the drag force can balance the Lorentz forces F_L of the driving current only if $F_L < F_{max}$ and $v < v_0$. At $v > v_0$ the velocity of a straight vortex driven by a uniform current density jumps to greater values corresponding to highly dissipative states [19]. Such LO instability has been observed on many superconducting materials [21–26] with typical values of $v_0 \sim 10^{-2} - 1$ km/s. At the LO instability, a differential flux-flow resistivity becomes negative, resulting in jumps and negative slopes on I-V curves.

An estimate of the maximum vortex velocity $v_m \sim \phi_0 B/\eta_0 \mu_0 \lambda$ in a Nb cavity at $B \approx 0.1 B_c \approx 20$ mT gives $v_m \approx 0.1 B_c \rho_n / \mu_0 \lambda B_{c2} \approx 1$ km/s which is larger than typical LO critical velocities $v_0 \approx 0.01 - 1$ km/s observed on Nb films [21]. Thus, for strong RF fields of interest to the Nb cavities, the Bardeen-Stephen model becomes inadequate and the velocity dependence of $\eta(v)$ should be taken into account.

The effective inertial mass m per unit length of the vortex in Eq. (1) mostly results from the kinetic energy of quasiparticles in the vortex core [20]. The first estimates of the vortex mass by Suhl [27] gave $m_s \approx 2k_F/\pi^3$, where m_e is the electron mass, $k_F = (3\pi^2 n_0)^{1/3}$ is the Fermi wave vector and n_0 is the electron density. Since then many different mechanisms have been proposed [28–30] which can increase the vortex mass well above the Suhl estimate. Measurements of the vortex mass in Nb by Golubchik et al., [31] have shown that m can be some 2 orders of magnitude higher than m_s near T_c .

DYNAMIC EQUATIONS

Combining all force contributions discussed above, we reduce Eq. (1) to a single nonlinear partial differential equation for the local displacement $u(z, t)$ of the vortex line written in the following dimensionless form:

$$m\ddot{u}\sqrt{1 + u'^2} + \frac{\gamma\dot{u}\sqrt{1 + u'^2}}{1 + \alpha\dot{u}^2(1 + u'^2)} = \frac{u''}{(1 + u'^2)^{3/2}} - \beta_1 e^{-z}, \quad (3)$$

where $u(z, t) = x(z, t)/\lambda$ is the dimensionless displacement of the vortex line along x , and the coordinate z and time t are in units of λ and the rf period, respectively. The parameters in Eq. (3) are given by

$$\gamma = f/f_0, \quad f_0 = B_{c1}\rho_n/B_{c2}\lambda^2\mu_0 \quad (4)$$

$$\alpha = \alpha_0\gamma^2, \quad \alpha_0 = (\lambda f_0/v_0)^2 \quad (5)$$

$$\beta_1 = \beta \sin(2\pi t), \quad \beta = B/B_{c1} \quad (6)$$

$$\mu = \mu_1\gamma^2, \quad \mu_1 = \lambda^2 f_0^2 m\mu_0/\phi_0 B_{c1}, \quad (7)$$

where B is the applied field, and $B_{c1} = (\phi_0/4\pi\lambda^2) \ln(\kappa + 0.5)$ is the lower critical field.

The RF power $P_0 = \tau_m^{-1} \int_0^{\tau_m} \int_0^l \eta v^2 dz dt$ produced by the drag force along the oscillating vortex and averaged over the time period τ_m can be expressed in terms of the dimensionless power P as follows

$$P = \frac{P_0}{P_1} = \gamma^2 \int_0^1 dt \int_0^l \frac{\dot{u}^2(1 + u'^2)^{3/2} dz}{1 + \alpha(1 + u'^2)\dot{u}^2}, \quad (8)$$

where $P_1 = \lambda^3 f_0^2 \eta_0$. We then define the dimensionless surface resistance $R_s(\beta)$ which gives the field dependence of the residual resistance of trapped vortices:

$$R_s(\beta) = P(\beta)/\beta^2. \quad (9)$$

NUMERICAL RESULTS

Equation (3) was simulated numerically with the boundary conditions $u'(0) = 0$ and $u(l) = 0$ using COMSOL [32]. Taking $\lambda/\xi = 1$, $\lambda = 40$ nm, $\rho_n = 10^{-9}$ Ωm , $n_0 = 6 \times 10^{28}$ m^{-3} [33], $f = 1$ GHz, 10 GHz, and $v_0 = 1 - 100$ m/s [23] for clean Nb at $T \ll T_c$, we obtain $\gamma \approx 0.01$ and 0.1 for 1 GHz and 10 GHz, respectively. Given the lack of experimental data for v_0 for Nb at $T \ll T_c$, we simulated Eq. (3) for different γ at $\alpha = 0, 1, 10$ and 100 which cover

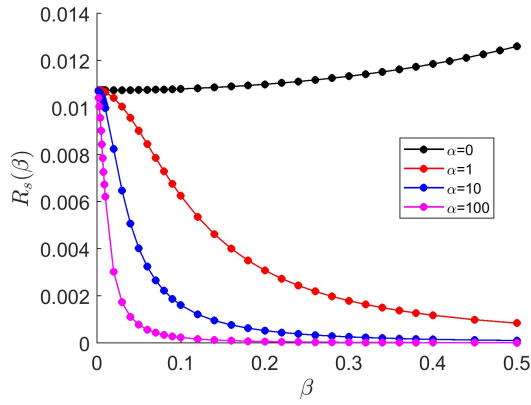


Figure 2: R_s vs β at $\gamma = 0.01$ for $l/\lambda = 3$.

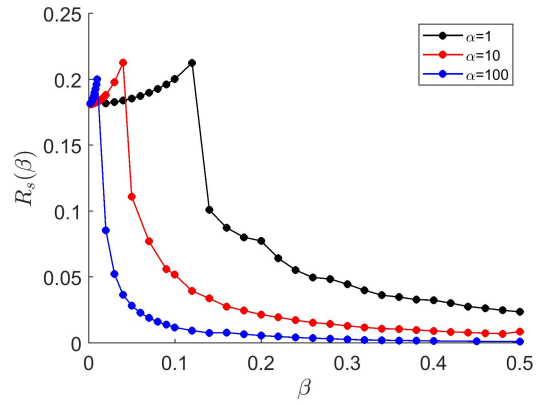


Figure 3: R_s vs β at $\gamma = 0.1$ for $l/\lambda = 3$.

the observed values of v_0 near T_c and the likely decrease of v_0 at low temperatures. We also set $\mu/\gamma = 10^{-4}$ by taking the vortex mass $m = 50 m_s \approx 2.5 \cdot 10^{-20}$ kg/m for Nb.

Shown in Figure 2 are the field dependencies of R_s calculated for different values of α at $\gamma = 0.01$. At low frequencies $\alpha \propto f^2 \ll 1$, the vortex velocities are small so the LO mechanism is ineffective, and the surface resistance increases with B as it is expected from the conventional Bardeen-Stephen viscous drag force and the effect of nonlinear vortex elasticity. However, as the frequency increases and α exceeds $\alpha_c \sim 1$, the surface resistance starts decreasing with B even at small fields due to the decrease of the LO vortex viscosity with v , as it is evident from Eq. (8).

If $\mu \ll \gamma \ll 1$, the first two terms in the left hand side of Eq. (3) are negligible and $u(z, t)$ can be obtained analytically. For instance, if $\alpha \dot{u}^2 \gg 1$, the velocity \dot{u} cancels out in Eq. (8) and $P \approx \gamma^2 l / \alpha$ becomes independent of β at $0.1 < \beta < 0.5$. In this case $R_s \approx \gamma^2 l / \alpha^2 \beta^2$ decreases with β in good agreement with the numerical result presented in Fig. 2. As the frequency increases the parameter $\alpha \propto f^2$ increases and the drop of $R_s(B)$ with B becomes more pronounced. Moreover, this dependence of $R_s \propto B^{-2}$ is in agreement with the experimental data on the low-field decrease of $R_s(B)$ observed on Nb cavities [34]. At low fields, $\beta \lesssim \sqrt{\alpha} / 2\pi l^2$ the surface resistance tends to a constant value, as shown in Fig. 2.

The dimensionless R_s can be converted back to Ωm^2 units by multiplying R_s by $2\mu_0^2 P_1 / B_{c1}^2 \approx 5 \cdot 10^{-16} \Omega\text{m}^2$ for a single trapped vortex in Nb. For $\gamma = 0.01$ and $\alpha = 100$, this gives $R_s \approx 120 \text{ n}\Omega\mu\text{m}^2$ at $\beta = 0.1$ and $R_s \approx 5200 \text{ n}\Omega\mu\text{m}^2$ at $\beta = 0.002$. The net residual resistance is then obtained by multiplying R_s by the mean areal density of trapped vortices.

Figure 2 shows the field dependence of R_s calculated at $\gamma = 0.1$ for different values of α . Unlike the case of $\gamma = 0.01$ considered above, the $R_s(\beta)$ curves at $\gamma = 0.1$ have nonmonotonic field dependencies, the peaks in $R_s(\beta)$ shifting to lower fields as the frequency and the parameter α increase.

The character of vortex oscillations changes significantly as β exceeds the peak position in $R_s(\beta)$. For instance, Fig. 4

shows the vortex tip oscillations near the peak of $R_s(\beta)$ in Fig. 3 for the case of $\gamma = 0.1$ and $\alpha = 10$. Clearly the time dependence of $u(0, t)$ changes from a nearly harmonic at β before the peak to a highly unharmonic $u(0, t)$ after the peak. This behavior can be qualitatively attributed to the fact that the velocity of the vortex tip reaches the LO instability threshold, which is however countered by the restoring elastic force due to the line tension of the rest of the vortex segment.

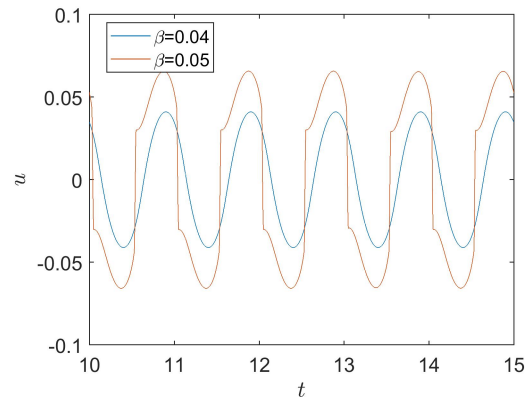


Figure 4: Vortex tip oscillation near the peak in Figure 3 for the case of $\gamma = 0.1$ and $\alpha = 10$. Here the blue and the red lines correspond to $u(0, t)$ just before and after the peak, respectively.

Another issue is that the vortex oscillations are mostly confined within the elastic skin depth $L_\omega \approx \sqrt{\epsilon/\eta(v)\omega}$ from the surface [6]. If $\gamma = 0.01$, the length $L_\omega \approx 10\lambda$ is larger than the simulated vortex length $l = 3\lambda$, so the vortex segment swings as a whole at all β . However, at $\gamma = 0.1$, the length $L_\omega \approx 3\lambda$ is about equal to l at $\beta \ll 1$. In this case R_s first increases as β increases, but after the peak in $R_s(\beta)$ at which F_η reaches the LO maximum, the viscous drag drops rapidly with v . As a result, L_ω becomes much larger than l , and $R_s(\beta)$ starts decreasing with β similar to the case shown in Fig. 2.

The parameters γ , α and μ depend on the concentration of nonmagnetic impurities which can be taken into account in the dependencies of $\rho_n \propto 1/l_i$, $\lambda \propto 1/\sqrt{l_i}$, $v_0 \propto \sqrt{l_i}$ and $\xi \propto \sqrt{l_i}$ on the mean-free path l_i in the dirty limit. In this case all γ , α and μ would increase like l_i^{-2} as l_i decreases. Therefore, $\gamma = 0.1$ can represent the case of a dirty surface layer of Nb at 1 GHz or at a pure Nb at 10 GHz.

The effect of frequency on the field dependence of R_s can be inferred from Figs. 2 and 3, since $\gamma \propto f$ and $\alpha \propto f^2$. For instance, Fig. 5 shows the change in the field dependence of $R_s(\beta, f)$ with frequency calculated for $\gamma = 0.01$ and $\alpha = 1$ at 1 GHz. In this case $R_s(\beta)$ is nearly field-independent at low f but as the frequency increases, a strong decrease of R_s with the RF field develops.

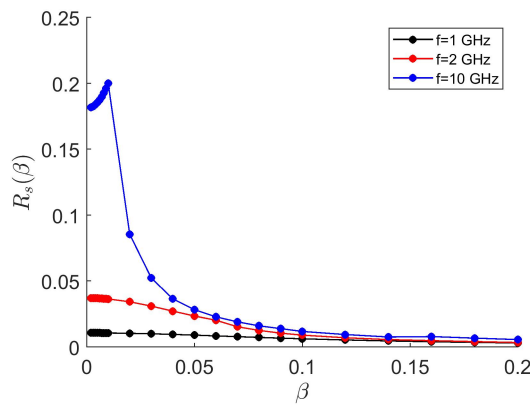


Figure 5: $R_s(\beta)$ vs β at $f = 1$ GHz, 2 GHz and 10 GHz.

The results presented in this work suggest that strong oscillations of trapped vortices can result in a decrease of the residual surface resistance with the RF field. This effect can contribute to the negative $Q(H)$ slope observed on nitrogen or titanium alloyed Nb cavities [35–39]. The vortex mechanism based on the LO decrease of the drag coefficient with the vortex velocity has a different physics than the decrease of the quasiparticle BCS surface resistance with the RF field [40, 41]. Yet our simulations show that trapped vortices could provide a field-induced reduction of the residual resistance which becomes more pronounced at higher frequencies. This result seems consistent with the recent experiment [42] which showed that a negative $Q(H)$ slope in nitrogen-doped Nb cavities becomes stronger as the RF frequency increases.

CONCLUSION

We presented extensive simulations of the nonlinear dynamics of a single vortex under strong rf magnetic field. The power dissipated by strongly oscillating vortex segment was calculated taking into account the nonlinear line tension of the vortex, nonlinear Larkin-Ovchinnikov viscous drag force and the vortex mass at different RF frequencies. At low frequencies $R_s(H)$ gradually increases with field, but as the frequency increases $R_s(H)$ becomes a non-monotonic function of H which decreases with H at higher fields. These

results suggest that trapped vortices could provide a field-induced reduction of the residual surface resistance which contributes to the extended $Q(H)$ rise observed on Nb cavities.

ACKNOWLEDGMENTS

This work was supported by NSF under Grant 100614-010 and Grant 1734075.

REFERENCES

- [1] H. Padamsee, J. Knobloch, and T. Hays, *RF Superconductivity for Accelerators*, Second Ed. Wiley ISBN: 978-3-527-40842-9, 2008.
- [2] C Z. Antoine, *Materials and Surface Aspects in the Development of SRF Niobium Cavities*, Institute of Electronic Systems, Warsaw University of Technology, 2012.
- [3] A. Gurevich, “Superconducting radio-frequency fundamentals for particle accelerators”, *Rev. Accel. Sci. Technol.*, vol. 5, pp. 119-146, 2012.
- [4] D.B. Liarte, D. Hall, P.N. Koufalas, A. Miyazaki, A. Senanian, M. Liepe, and J.P. Sethna, “Vortex dynamics and losses due to pinning: Dissipation from trapped magnetic flux in resonant superconducting radio-frequency cavities”, *Phys. Rev. Applied*, vol. 10, pp. 054057, 2018.
- [5] J.-M. Vogt, O. Kugeler, and J. Knobloch, “Impact of cool-down conditions at T_c on the superconducting rf cavity quality factor”, *Phys. Rev. ST Accel. Beams*, vol. 16, pp. 102002, 2013.
- [6] A. Gurevich and G. Ciovati, “Effect of vortex hotspots on the radio-frequency surface resistance of superconductors”, *Phys. Rev. B*, vol. 87, pp. 054502, 2013.
- [7] A. Romanenko, A. Grassellino, O. Melnychuk, and D.A. Sergatskov, “Dependence of the residual surface resistance of superconducting radio frequency cavities on the cooling dynamics around T_c ”, *J. Appl. Phys.*, vol. 115, pp. 184903, 2014.
- [8] D. Gonnella, R. Eichhorn, F. Furuta, M. Ge, D. Hall, V. Ho, G. Hoffstaetter, M. Liepe, T. O’Connell, S. Posen, P. Quigley, J. Sears, V. Veshcherevich, A. Grassellino, A. Romanenko, and D.A. Sergatskov, “Nitrogen-doped 9-cell cavity performance in a test cryomodule for LCLS-II”, *J. Appl. Phys.*, vol. 117, pp. 023908, 2015.
- [9] M. Martinello, M. Checchin, A. Grassellino, A.C. Crawford, O. Melnychuk, A. Romanenko, and A.D. Sergatskov, “Magnetic flux studies in horizontally cooled elliptical superconducting cavities”, *J. Appl. Phys.*, vol. 118, pp. 044505, 2015.
- [10] J.-M. Vogt, O. Kugeler, and J. Knobloch, “High-Q operation of superconducting rf cavities: Potential impact of thermocurrents on the rf surface resistance”, *Phys. Rev. ST Accel. Beams*, vol. 18, pp. 042001, 2015.
- [11] H. Huang, T. Kubo, and R.L. Geng, “Dependence of trapped-flux-induced surface resistance of a large-grain Nb superconducting radio-frequency cavity on spatial temperature gradient during cooldown through T_c ”, *Phys. Rev. Accel. Beams*, vol. 19, pp. 082001, 2016.

- Content from this work may be used under the terms of the CC BY 3.0 licence (© 2019). Any distribution of this work must maintain attribution to the author(s), title of the work, publisher, and DOI.
- [12] S. Posen, M. Checchin, A.C. Crawford, A. Grassellino, M. Martinello, O.S. Melnychuk, A. Romanenko, D.A. Sergatskov, and Y. Trenikhina, “Efficient expulsion of magnetic flux in superconducting radiofrequency cavities for high Q_0 applications”, *J. Appl. Phys.*, vol. 119, pp. 213903, 2016.
- [13] D. Gonnella, J. Kaufman, and M. Liepe, “Impact of nitrogen doping of niobium superconducting cavities on the sensitivity of surface resistance to trapped magnetic flux”, *J. Appl. Phys.*, vol. 119, pp. 073904, 2016.
- [14] E.H. Brandt, “The flux-line lattice in superconductors”, *Rep. Progr. Phys.*, vol. 58, pp. 1465, 1995.
- [15] M. Checchin, M. Martinello, A. Grassellino, A. Romanenko, and J.F. Zasadzinski, “Electron mean free path dependence of the vortex surface impedance”, *Supercond. Sci. Technol.*, vol. 30, pp. 034003, 2017.
- [16] A. Gurevich and G. Ciovati, “Dynamics of vortex penetration, jumpwise instabilities, and nonlinear surface resistance of type-II superconductors in strong rf fields”, *Phys. Rev. B*, vol. 77, pp. 104501, 2008.
- [17] W.-K. Kwok, U. Welp, A. Glatz, A.E. Koshelev, K.J. Kihlstrom, and G.W. Crabtree, “Vortices in high-performance high-temperature superconductors.”, *Rep. Progr. Phys.*, vol. 79, pp. 116501, 2016.
- [18] M. Tinkham, *Introduction to superconductivity*, Courier Corporation, 2004.
- [19] A.I. Larkin and Yu.N. Ovchinnikov, “Nonlinear conductivity of superconductors in the mixed state”, *J. Exp. Theor. Phys.*, vol. 41, pp. 960-965, 1975.
- [20] N.B. Kopnin, *Theory of nonequilibrium superconductivity*, Oxford University Press, 2001.
- [21] A.A. Armenio, C. Bell, J. Aarts, and C. Attanasio, “High-velocity instabilities in the vortex lattice of Nb/permalloy bilayers”, *Phys. Rev. B*, vol. 76, pp. 054502, 2007.
- [22] C. Villard, C. Peroz, and A. Sulpice, “Viscous motion of vortices in superconducting niobium films”, *J. Low Temp. Phys.*, vol. 131, pp. 957–961, 2003.
- [23] G. Grimaldi, A. Leo, A. Nigro, S. Pace, A.A. Angrisani, and C. Attanasio, “Flux flow velocity instability in wide superconducting films”, *J. Phys: Conference Series*, vol. 97, pp. 012111, 2008.
- [24] S.G. Doettinger, R.P. Huebener, R. Gerdemann, A. Kühle, S. Anders, T.G. Träube, and J.C. Villèger, “Electronic Instability at High Flux-Flow Velocities in High- T_c Superconducting Films”, *Phys. Rev. Lett.*, vol. 73, pp. 1691, 1994.
- [25] A.V. Samoilov, M. Konczykowski, N.-C. Yeh, S. Berry, and C.C. Tsuei, “Electric-Field-Induced Electronic Instability in Amorphous Mo_3Si Superconducting Films”, *Phys. Rev. Lett.*, vol. 75, pp. 4118, 1995.
- [26] M. Kunchur, B.I. Ivlev, and J.M. Knight, “Steps in the Negative-Differential-Conductivity Regime of a Superconductor”, *Phys. Rev. Lett.*, vol. 87, pp. 177001, 2001.
- [27] H. Suhl, “Inertial mass of a moving fluxoid”, *Phys. Rev. Lett.*, vol. 14, pp. 226, 1965.
- [28] N.B. Kopnin V.M. and Vinokur, “Dynamic Vortex Mass in Clean Fermi Superfluids and Superconductors”, *Phys. Rev. Lett.*, vol. 81, pp. 3952, 1998.
- [29] E.M. Chudnovsky and A.B. Kuklov, “Inertial Mass of the Abrikosov Vortex”, *Phys. Rev. Lett.*, vol. 91, pp. 067004, 2003.
- [30] J.H. Han, J.S. Kim, M.J. Kim, and P. Ao, “Effective vortex mass from microscopic theory”, *Phys. Rev. B*, vol. 71, pp. 125108, 2005.
- [31] D. Golubchik, E. Polturak, and G. Koren, “Mass of a vortex in a superconducting film measured via magneto-optical imaging plus ultrafast heating and cooling”, *Phys. Rev. B*, vol. 85, pp. 060504, 2012.
- [32] COMSOL Multiphysics Modeling Software, <https://www.comsol.com>
- [33] N.W. Ashcroft and N.D. Mermin, *Solid state physics*, 1976.
- [34] G. Ciovati, “Effect of low-temperature baking on the radio-frequency properties of niobium superconducting cavities for particle accelerators”, *J. Appl. Phys.*, vol. 96, pp. 1591, 2004.
- [35] P. Dhakal, G. Ciovati, G.R. Myneni, K.E. Gray, N. Groll, P. Maheshwari, D.M. McRae, R. Pike, T. Proslie, F. Stevie, R.P. Walsh, Q. Yang, and J. Zasadzinski, “Effect of high temperature heat treatments on the quality factor of a large-grain superconducting radio-frequency niobium cavity”, *Phys. Rev. ST Accel. Beams*, vol. 16, pp. 042001, 2013.
- [36] A. Grassellino, A. Romanenko, D. Sergatskov, O. Melnychuk, Y. Trenikhina, A. Crawford, A. Rowe, M. Wong, T. Khabiboulline, and F. Barkov, “Nitrogen and argon doping of niobium for superconducting radio frequency cavities: a pathway to highly efficient accelerating structures”, *Supercond. Sci. Technol.*, vol. 26, pp. 102001, 2013.
- [37] G. Ciovati, P. Dhakal, and A. Gurevich, “Decrease of the surface resistance in superconducting niobium resonator cavities by the microwave field”, *Appl. Phys. Lett.*, vol. 104, pp. 092601, 2014.
- [38] G. Ciovati, P. Dhakal, and G.R. Myneni, “Superconducting radio-frequency cavities made from medium and low-purity niobium ingots”, *Supercond. Sci. Technol.*, vol. 29, pp. 064002, 2016.
- [39] A. Grassellino, A. Romanenko, Y. Trenikhina, M. Checchin, M. Martinello, O.S. Melnychuk, S. Chandrasekaran, D.A. Sergatskov, S. Posen, A.C. Crawford, S. Aderhold, and D. Bice, “Unprecedented quality factors at accelerating gradients up to 45 MVm^{-1} in niobium superconducting resonators via low temperature nitrogen infusion”, *Supercond. Sci. Technol.*, vol. 30, pp. 094004, 2017.
- [40] A. Gurevich, “Reduction of dissipative nonlinear conductivity of superconductors by static and microwave magnetic fields”, *Phys. Rev. Lett.*, vol. 113, pp. 087001, 2014.
- [41] A. Gurevich, “Theory of RF superconductivity for resonant cavities”, *Supercond. Sci. Technol.*, vol. 30, pp. 034004, 2017.
- [42] M. Martinello, M. Checchin, A. Romanenko, A. Grassellino, S. Aderhold, S.K. Chandrasekaran, O. Melnychuk, S. Posen, and D.A. Sergatskov, “Field-Enhanced Superconductivity in High-Frequency Niobium Accelerating Cavities”, *Phys. Rev. Lett.*, vol. 121, pp. 224801, 2018.